ResearchGate

See discussions, stats, and author profiles for this publication at: https://www.researchgate.net/publication/235794141

Dynamic Trap Formation and Elimination in Colloidal Quantum Dots

ARTICLE *in* JOURNAL OF PHYSICAL CHEMISTRY LETTERS · MARCH 2013

Impact Factor: 7.46 · DOI: 10.1021/jz400125r

CITATIONS
38

READS
21

4 AUTHORS, INCLUDING:

Oleksandr Voznyy
University of Toronto
75 PUBLICATIONS **1,683** CITATIONS

SEE PROFILE

Edward H Sargent
University of Toronto
417 PUBLICATIONS **13,830** CITATIONS

SEE PROFILE

Available from: Edward H Sargent
Retrieved on: 27 January 2016

THE JOURNAL OF PHYSICAL CHEMISTRY Letters

Letter

pubs.acs.org/JPCL

Dynamic Trap Formation and Elimination in Colloidal Quantum Dots

O. Voznyy, S. M. Thon, A. H. Ip, and E. H. Sargent*

Department of Electrical and Computer Engineering, University of Toronto, 10 King's College Road, Toronto, Ontario, M5S 3G4, Canada

Supporting Information

ABSTRACT: Using first-principles simulations on PbS and CdSe colloidal quantum dots, we find that surface defects form in response to electronic doping and charging of the nanoparticles. We show that electronic trap states in nanocrystals are dynamic entities, in contrast with the conventional picture wherein traps are viewed as stable electronic states that can be filled or emptied, but not created or destroyed. These traps arise from the formation or breaking of atomic dimers at the nanoparticle surface. The dimers' energy levels can reside within the bandgap, in which case a trap is formed. Fortunately, we are also able to identify a number of shallow-electron-affinity cations that stabilize the surface, working to counter dynamic trap formation and allowing for trap-free doping.

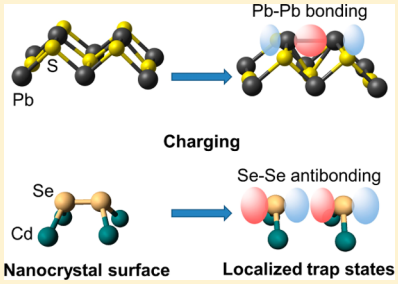

SECTION: Physical Processes in Nanomaterials and Nanostructures

Colloidal quantum dots (CQDs) have found applications in communications, lighting, lasers, biomedical imaging, and photovoltaics in view of the tunability of their optical and electronic properties and the advantage of their low-cost large-area processing.[1−5] The optical and electronic properties of CQDs are degraded by the presence of shallow and deep electronic trap states. Deep traps lead to nonradiative recombination pathways that can lower photoemission quantum yields[5] and produce intermittent blinking.[6−8] Trap states militate against efficient charge carrier extraction from CQD films even when present at small concentrations.[9] Reducing the trap state energy depth and volume density represents one of the most important avenues to improving the transport properties of CQD film devices and CQD-based solar cells in particular.[2,10]

The origins of electronic traps in CQD films may be partially attributed to present-day fabrication techniques, wherein the long alkane ligands required for colloidal stability are replaced with shorter organic[4,11−13] or inorganic ones.[14−16] This modification of the surface − especially if incomplete or suboptimal − may be a source of surface defects. A substantial density of deep traps in PbS CQD films is observed in photoluminescence[10,17,18] and photoconductivity measurements using optical field-effect transistors.[19] Previously, we reported the formation of trap states following the reduction of surface ligand coverage.[10,20] Desorption of ligands reduces the coordination of the surface atoms, leading, as expected, to traps. At the same time, the stoichiometry of the CQD changes leading to electronic doping.[20]

Here we show that electronic doping of PbS and CdSe quantum dots also leads to surface defect formation, even in the case of idealized surface geometries. The resultant formation of electronic traps that require filling thus militates against the creation of a substantial free carrier density in the bandedge states. It instead pins the Fermi level near the trap level. Such self-compensation, which opposes net doping during crystal growth, is also known in bulk and thin film semiconductors.[21] Defects, such as vacancies or interstitials, form in the bulk material itself, irrespective of the chemical nature of the dopant, and to remedy those defects, an appropriate choice of the growth conditions is required.

Formation of defects is much less energetically costly on surfaces than in the bulk, making nanocrystals more prone to self-compensating defects. Herein we find that in nanocrystals, defects may form not only during growth but also may occur and disappear dynamically in a fully formed nanocrystal. This can be triggered by changes in the population of charge carriers in a band, such as via charging, doping, or even photoexcitation.

Since this in situ formation of traps in quantum dots will work counter to performance and stability, we explore new strategies that prevent the formation of traps even in doped CQDs. We find specifically that terminating surfaces using cations having an electron affinity shallower than the quantum dot's bandgap leads to a stable and trap-free bandgap.

We began by investigating PbS CQDs and employed Pb-rich stoichiometries observed experimentally.[22] When we assumed the idealized geometries (see Computational Methods), and when we chose the number of ligands to satisfy electronic balance,[20] we achieved trap-free nanocrystals (Figure 1a). The projected density of states (PDOS) shows that the valence band is formed mainly from chalcogenide and halogen orbitals, while the conduction band is formed from Pb orbitals; the Fermi level lies in the midgap. The sufficiency of these conditions to achieve trap-free nanocrystals agrees well with previously reported studies of CdSe passivated with oleic acid[23] and PbS terminated with thiol[10] ligands.

Received: January 18, 2013
Accepted: March 6, 2013
Published: March 6, 2013

 © 2013 American Chemical Society

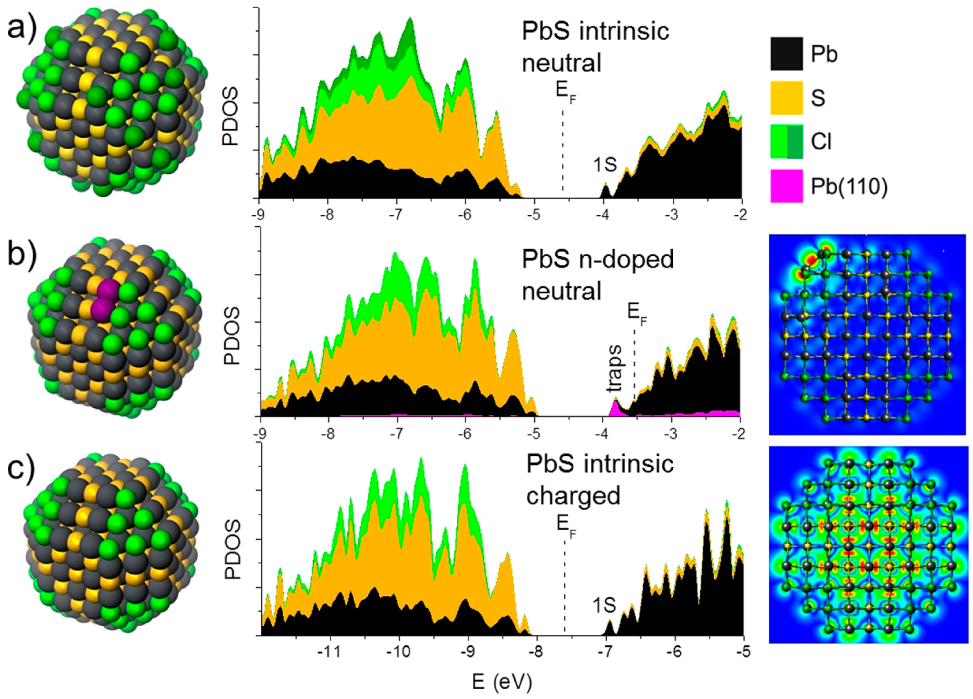

Figure 1. Structures of the PbS CQDs used in calculations with corresponding projected densities of states and spatial charge densities of the lowest energy state on the conduction band side: (a) electronically balanced dot, (b) doped dot due to removal of halide ligands from (110) facets (dark green) resulting in formation of Pb dimers (purple) and localization of charge on them (right panel), (c) positively charging the dot in panel b eliminates the dimers and results in a delocalized state. PDOS energies are referenced to vacuum level.

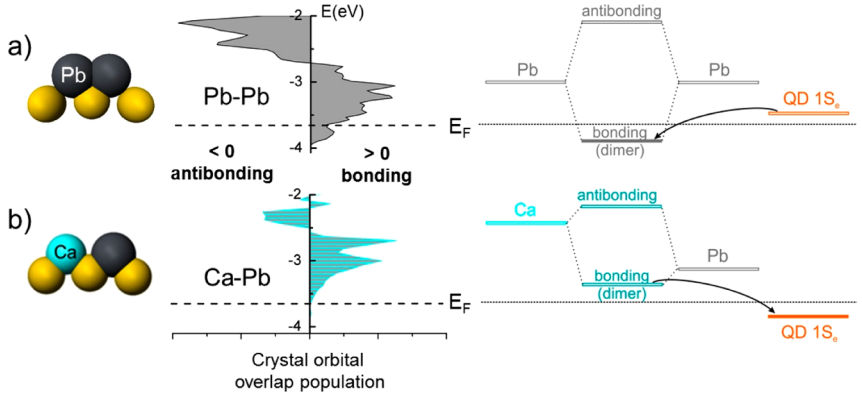

Figure 2. COOP analysis in n-doped PbS CQDs: (a) low-lying Pb−Pb bonding orbitals leading to dimer formation and (b) replacement of Pb with a cation with smaller electron affinity shifts the bonding orbitals upward in energy, avoiding their population.

We then turned to exploring conditions in which n-type doping can be achieved. We remove all ligands from (110) facets without adjusting the net charge of the CQD. This leads to an excess of electrons in the conduction band, i.e., electronic doping. It also leads to the formation of Pb dimers on (110) facets and a strong PDOS contribution to the lowest conduction band states from these dimers (Figure 1b). Investigation of the wave functions confirms that the lowest conduction band states are traps, strongly localized on the newly formed Pb dimers. To check whether these traps were formed not due to undercoordination of the surface Pb atoms, but due to electronic doping itself, we imposed a positive charge on the structure to shift the Fermi level back to the midgap. We found that bringing the nanocrystal to an intrinsic state led to elimination of both the dimers and the trap states (Figure 1c). This confirms that the traps and dimer formation arise due to the doping itself.

It is surprising that this association of cation dimers on the surface with traps has not previously been reported. We investigated the charged CQD in a geometry without Pb dimers, and found that it is a local energy minimum, suggesting an explanation for why this effect went unnoticed previously. Several molecular dynamics steps allow for a transition to a dimerized configuration, suggestive of a small energetic barrier between the two configurations. Subsequent geometry optimization confirms the stabilization by 0.2 eV per dimer. The degree of doping is also important for dimer formation. We find that three to four excess electrons are required to induce one dimer. Such a degree of charge imbalance is not implausible during CQD synthesis, as every excess cation in a nanocrystal of ∼1000 atoms brings two excess electrons. This, however, does not necessarily contribute to a high doping level in the CQD ensemble, as not every dot needs to be off-balance.

dx.doi.org/10.1021/jz400125r | J. Phys. Chem. Lett. 2013, 4, 987−992

Moreover, these excess electrons become trapped and thus do not contribute to measured free carrier density.

To investigate the reason for charging-activated trap formation, we carried out crystal overlap orbital population (COOP) analysis for pairs of Pb atoms on (110) facets. These atom pairs are particularly prone to dimerization. The sign of COOP curves distinguishes between orbital bonding and antibonding interactions. We find that, irrespective of the doping level, bonding Pb−Pb orbitals are available right at the bottom of the conduction band (Figure 2a). As soon as electrons are available to populate those orbitals, the bond can form, leading to formation of a dimer.

To verify whether the energetic position of the dimer orbitals remains fixed relative to vacuum, or, in the alternative hypothesis, fixed relative to a bandedge, we performed COOP analysis for bulk PbS (Figure S3). We found that dimer orbitals moved in concert with the bandedge, thus, dynamic trap formation remains relevant for a wide range of nanocrystals sizes. Test simulations on 3 and 6 nm nanocrystals confirmed the dimer formation.

We sought means to avoid the formation of dimers. We took the approach of seeking to shift the Pb−Pb bonding orbitals higher in energy. The most straightforward way to achieve this is to passivate Pb with Cl. Simulations confirm that dimers can be eliminated this way. However, addition of extra Cl ligands changes the overall stoichiometry of the nanocrystal, resulting in reduced n-type doping. This strategy, while beneficial in the control over trap states, does not achieve the goal of simultaneously trap-free and strongly net-doped nanocrystals.

We explored the alternative possibility of shifting the dimer orbitals upward in energy by replacing dimerization-prone Pb with other cations. We started with Cd, which is often deployed in a wider-bandgap CdS shell on PbS CQDs, suggesting that Cd could potentially have a higher orbital energy compared to Pb. Incorporation of Cd on the surface even in minute amounts was shown to reduce the trap density and increase the photovoltaic performance in previous experimental reports.[10,16] It had also been observed to improve transport properties in PbS CQD films employing inorganic ligands.[14]

Simulations reveal that Cd stability on the PbS surface is strongly dependent on the charge balance of the dot: it is stable on an intrinsic dot; however, if the dot is n-doped, Cd tends to desorb from the surface. Weak binding of Cd to PbS CQDs has previously been reported.[24] Expulsion of Cd atoms was also observed on unreconstructed CdSe (111) surfaces[25] and noted in our previous CdSe CQDs studies.[23] A similar balance-dependence of binding energies of organic molecules on GaAs surfaces is also known.[26] Desorption of Cd provides another self-compensation mechanism in doped PbS CQDs. In contrast to the dimerization of surface Pb, which leads to trap formation, expulsion of Cd reduces the number of cations in the quantum dot, reinstating the charge balance and eliminating the traps.

In sum, as seen above in the case of adsorption of extra halide ligands on Pb dimers, the desired reduction in trap density comes at the cost of reduced net doping. Nonetheless, cadmium desorption does suggest a convenient self-regulating strategy to achieve intrinsic CQDs having a low number of deep traps.

We expected that cations with a shallower electron affinity would have orbitals positioned higher than those of Pb when adsorbed on the PbS surface. This, we posited, could depopulate the bonding orbitals, and thus prevent dimer formation. Alkali and alkali-earth metals are good candidates for this purpose. We explored Ca and Ba cations, which share the same oxidation state (+2) as Pb in our CQDs. Additionally, Ca and Ba are known to form stable sulfides in a rocksalt structure, the same lattice configuration as PbS. We were also encouraged by the distinctively high photoluminescence quantum yield of Ca-treated PbS CQDs in a recent report.[14]

Our results show that using Ca to replace the Pb atoms on the dimerization-prone (110) facets (Figure 2b) prevented dimerization while preserving doping. Calcium is found to stabilize at the same site as Pb, supporting the rocksalt structure. The binding energy of Ca bound to two S atoms and two halogens is calculated to be 1.95 eV, slightly lower than 2.3 eV for Pb in the same position. Similar studies employing Ba produced the same behavior. Since the atomic radius of Ba is substantially larger than that of Pb, this confirms that dimerization is not a geometric but instead an electronic effect. Figure 2b shows that the Ca−Pb bonding orbital is shifted upward in energy: as a consequence, it remains above the Fermi level even in doped nanocrystals.

We screened a range of cations employing the same full nanocrystals geometry to test whether electron affinity can be used as a predictive figure of merit for dimer elimination (Table 1). In general, we see a correlation between electron affinity and dimer formation. In the case of Ga, Pb−Ga dimer levels form localized states deep inside the conduction band, in contrast to being situated within the bandgap in bulk PbSe.[27] We believe that quantum confinement is responsible for pushing the Ga states out of the bandgap. These states, however, lie above the Fermi level and thus would not contribute to trapping, at least under low doping conditions. We also noted that, in some cases, cation-related states form in the gap in spite of the absence of dimerization (Cu).

Table 1. Effect of Different Cations Replacing Pb on Elimination of Electronic Traps and Dimers

cation	electron affinity	geometry	traps	cation orbital position
Cd	0	desorbs		
Zn	0	dimer, sp^2	deep	near VB
Ca	0.02	preserved		inside CB
Ba	0.14	preserved		inside CB
Na	0.55	preserved		inside CB
Ga	0.43	dimer, sp^2	above E_F	inside CB
Fe	0.15	unstable	deep	near CB
Pb	0.36	dimer	deep	near CB
Sn	1.11	dimer	deep	near CB
Cu	1.23	preserved	deep	near VB

Formation of charge-sensitive defects is ubiquitous in quantum dots and is not limited to the PbS material system. Our simulations of CdSe nanocrystals following published protocols[23,28−30] show that dimerization of Se anions on the surface is a common motif in both zincblende (Figure 3) and wurtzite (Figure S4) structures. In fact, the Se dimerization provides a convenient way to passivate Cd atoms on (001) facets possessing two dangling bonds − it is as stable as passivation via the oleic acid ligands. Anion dimerization is also a typical reconstruction of III−V and II−VI semiconductor surfaces.[31] In contrast to cation dimers in PbS, anion dimer bonding orbitals are positioned deep in the valence band. Se dimer antibonding states, however, are situated close to conduction band edge. It is these states that become populated and lead to dimer breaking and trap formation in response to

dx.doi.org/10.1021/jz400125r | J. Phys. Chem. Lett. 2013, 4, 987−992

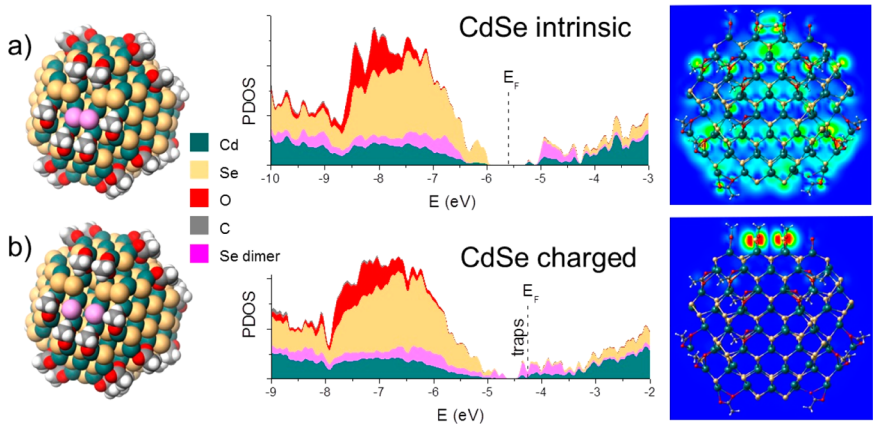

Figure 3. Formation of deep traps in oleic acid capped zincblende CdSe CQDs due to Se dimer breaking: (a) structure schematic, projected density of states plot, and spatial electron density map for an electronically balanced dot, and (b) the same plots for a negatively charged dot with the lowest-lying conduction band state localized on a broken dimer.

charging (Figure 3b), requiring only one or two excess electrons for trap formation. Cation dimerization, akin to that in PbS, is much rarer in tetrahedrally coordinated structures (CdSe), as such dimerization would infer high strains in view of cations' propensity for sp^2 hybridization on the surface.[23,28,29]

In Si nanoclusters, a preference for dimerization over passivation by hydrogen has been reported.[32] Our simulations (Figure S5) show that Si antibonding orbitals are located deep in the conduction band, and thus Si dimers remain stable even in charged nanocluster, in contrast to Se dimers in CdSe. Understanding the origin of the dynamic traps presented here should help develop strategies for trap elimination in CdSe, similar to solutions proposed above for PbS.

In conclusion, our computational studies reveal that semiconductor CQDs self-compensate in response to doping, effectively pinning the Fermi level inside the quantum-confined bandgap. They do so via the formation of surface defects that result in strongly localized states. In n-doped PbS, Pb dimers form, whereas in n-doped CdSe, electronic traps arise due to broken Se dimers.

Such defects can also form dynamically in response to charging. This observation is specific to nanocrystals, as it is unobserved in bulk systems, even those prone to self-compensation. We expect that populating the conduction band states via light excitation can also lead to trap formation, providing an atomistic example of light-activated traps that are called for in phenomenological models of blinking.[6−8] Similarly, the dynamic traps reported herein can offer an explanation for drain−source current decay under pulsed gate voltage in CQD field-effect transistors which cannot be explained solely by static traps.[11,33]

To avoid trap formation, it is sufficient to restore the charge balance of the CQD via control over stoichiometry. For doped nanocrystals this can be done by altering the number of ligands or the excess of cations. When net doping is desired, a novel chemical modification is required. We have demonstrated that the introduction of new atomic species on the surface can be deployed to destabilize the defects, ensuring that excess electrons populate quantum-confined conduction band states before they reach the trap states.

■ COMPUTATIONAL METHODS

Simulations were performed using SIESTA software[34] employing strictly localized numerical atomic orbitals in the pseudopotential approach. We used the relativistic Troullier-Martins pseudopotentials with nonlinear core corrections and the generalized gradient approximation in the Perdew−Burke−Ernzerhoff formulation throughout. Charge density was represented on a grid with 200 Ry effective cutoff.

Nanocrystal cores 1.5−2.4 nm in diameter (up to ∼400 atoms) were prepared by carving a sphere from bulk rocksalt, wurtzite, and zincblende structures. Striving for idealized geometries, and following previous work,[23,35] we discarded all single-bonded atoms, resulting in well-defined facets in the (100), (110), and (111) crystallographic orientations. This choice of faceting is well justified since adsorption of adatoms or ligands on (100) rocksalt and (111) zincblende facets is less energetically favorable (Figure S1), while diffusion of ligands and adatoms on surface is well-known[23,36] and allows for stabilization in higher-coordinated geometries.

High ligand coverage (to cover all surface atoms with two and more dangling bonds) was imposed since the number of ligands is a key determinant of the charge balance in CQDs.[20] Oleic acid ligands, which are often used in the synthesis of both PbS[37] and CdSe,[38] were represented by a shorter acetate, deprotonated to allow for covalent binding.[39] We also tested halide ligands used in alternative syntheses.[10,16,40−43] Our simulations show that chlorine as a ligand is quite similar electronically to oleic acid (Figure S2), and we use Cl in all our further simulations as a less computationally demanding alternative. Full geometry relaxation was performed for each structure without imposing any symmetry constraints, until forces on atoms converged to 40 meV/Å.

■ ASSOCIATED CONTENT

Supporting Information

Full simulation input files and optimized geometries, comparison of halogen and carboxy ligands, results for Si and wurtzite CdSe. This material is available free of charge via the Internet at http://pubs.acs.org.

■ AUTHOR INFORMATION

Corresponding Author

*E-mail: ted.sargent@utoronto.ca.

Notes

The authors declare no competing financial interest.

■ ACKNOWLEDGMENTS

This publication is based in part on work supported by Award KUS-11-009-21, made by King Abdullah University of Science and Technology (KAUST), by the Ontario Research Fund Research Excellence Program, and by the Natural Sciences and Engineering Research Council (NSERC) of Canada. Computations were performed on the GPC supercomputer at the SciNet HPC Consortium.[44] SciNet is funded by the Canada Foundation for Innovation under the auspices of Compute Canada, the Government of Ontario, the Ontario Research Fund - Research Excellence, and the University of Toronto.

■ REFERENCES

(1) Klimov, V. I.; Ivanov, S. A.; Nanda, J.; Achermann, M.; Bezel, I.; McGuire, J. A.; Piryatinski, A. Single-exciton Optical Gain in Semiconductor Nanocrystals. *Nature* **2007**, *447*, 441−446.

(2) Kramer, I. J.; Sargent, E. H. Colloidal Quantum Dot Photovoltaics: A Path Forward. *ACS Nano* **2011**, *5*, 8506−8514.

(3) Yu, K.; Ouyang, J.; Zhang, Y.; Tung, H.-T.; Lin, S.; Nagelkerke, R. a L.; Kingston, D.; Wu, X.; Leek, D. M.; Wilkinson, D.; et al. Low-Temperature Noninjection Approach to Homogeneously-alloyed $PbSe_xS_{1-x}$ Colloidal Nanocrystals for Photovoltaic Applications. *ACS Appl. Mater. Interfaces* **2011**, *3*, 1511−1520.

(4) Pattantyus-Abraham, A. G.; Kramer, I. J.; Barkhouse, A. R.; Wang, X.; Konstantatos, G.; Debnath, R.; Levina, L.; Raabe, I.; Nazeeruddin, M. K.; Grätzel, M.; et al. Depleted-Heterojunction Colloidal Quantum Dot Solar Cells. *ACS Nano* **2010**, *4*, 3374−3380.

(5) Talapin, D. V; Lee, J.-S.; Kovalenko, M. V; Shevchenko, E. V Prospects of Colloidal Nanocrystals for Electronic and Optoelectronic Applications. *Chem. Rev.* **2010**, *110*, 389−458.

(6) Cordones, A. A.; Bixby, T. J.; Leone, S. R. Evidence for Multiple Trapping Mechanisms in Single CdSe/ZnS Quantum Dots from Fluorescence Intermittency Measurements over a Wide Range of Excitation Intensities. *J. Phys. Chem. C* **2011**, *115*, 6341−6349.

(7) Galland, C.; Ghosh, Y.; Steinbrück, A.; Hollingsworth, J. a; Htoon, H.; Klimov, V. I. Lifetime Blinking in Nonblinking Nanocrystal Quantum Dots. *Nat. Commun.* **2012**, *3*, 908.

(8) Frantsuzov, P.; Volkan-Kacso, S.; Janko, B. Universality of the Fluorescence Intermittency in Nanoscale Systems: Experiment and Theory. *Nano Lett* **2013**, *13*, 402−408.

(9) Zhitomirsky, D.; Kramer, I. J.; Labelle, A. J.; Fischer, A.; Debnath, R.; Pan, J.; Bakr, O. M.; Sargent, E. H. Colloidal Quantum Dot Photovoltaics: The Effect of Polydispersity. *Nano Lett.* **2012**, *12*, 1007−1012.

(10) Ip, A. H.; Thon, S. M.; Hoogland, S.; Voznyy, O.; Zhitomirsky, D.; Debnath, R.; Levina, L.; Rollny, L. R.; Carey, G. H.; Fischer, A.; et al. Hybrid Passivated Colloidal Quantum Dot Solids. *Nat. Nanotech.* **2012**, *7*, 577−582.

(11) Luther, J. M.; Law, M.; Song, Q.; Perkins, C. L.; Beard, M. C.; Nozik, A. J. Structural, Optical, and Electrical Properties of Self-Assembled Films of PbSe Nanocrystals Treated with 1,2-Ethanedithiol. *ACS Nano* **2008**, *2*, 271−280.

(12) Law, M.; Luther, J. M.; Song, Q.; Hughes, B. K.; Perkins, C. L.; Nozik, A. J. Structural, Optical, and Electrical Properties of PbSe Nanocrystal Solids Treated Thermally or with Simple Amines. *J. Am. Chem. Soc.* **2008**, *130*, 5974−5985.

(13) Ma, W.; Luther, J. M.; Zheng, H.; Wu, Y. Alivisatos, a P. Photovoltaic Devices Employing Ternary PbSxSe1-x Nanocrystals. *Nano Lett.* **2009**, *9*, 1699−1703.

(14) Nag, A.; Chung, D. S.; Dolzhnikov, D. S.; Dimitrijevic, N. M.; Chattopadhyay, S.; Shibata, T.; Talapin, D. V The Effect of Metal Ions on Photoluminescence, Charge Transport, Magnetic and Catalytic Properties of All-inorganic Colloidal Nanocrystals and Nanocrystal Solids. *J. Am. Chem. Soc.* **2012**, *134*, 13604−13615.

(15) Kovalenko, M. V; Scheele, M.; Talapin, D. V Colloidal Nanocrystals with Molecular Metal Chalcogenide Surface Ligands. *Science* **2009**, *324*, 1417−1420.

(16) Tang, J.; Kemp, K. W.; Hoogland, S.; Jeong, K. S.; Liu, H.; Levina, L.; Furukawa, M.; Wang, X.; Debnath, R.; Cha, D.; et al. Colloidal-Quantum-Dot Photovoltaics Using Atomic-Ligand Passivation. *Nat. Mater.* **2011**, *10*, 765−771.

(17) Nelson, C. A.; Zhu, X. Reversible Surface Electronic Traps in PbS Quantum Dot Solids Induced by an Order−Disorder Phase Transition in Capping Molecules. *J. Am. Chem. Soc.* **2012**, *134*, 7592−7595.

(18) Jeong, K. S.; Tang, J.; Liu, H.; Kim, J.; Schaefer, A. W.; Kemp, K.; Levina, L.; Wang, X.; Hoogland, S.; Debnath, R.; et al. Enhanced Mobility-Lifetime Products in PbS Colloidal Quantum Dot Photovoltaics. *ACS Nano* **2012**, *6*, 89−99.

(19) Nagpal, P.; Klimov, V. I. Role of Mid-gap States in Charge Transport and Photoconductivity in Semiconductor Nanocrystal Films. *Nat. Commun.* **2011**, *2*, 486.

(20) Voznyy, O.; Zhitomirsky, D.; Stadler, P.; Ning, Z.; Hoogland, S.; Sargent, E. H. A Charge-Orbital Balance Picture of Doping in Colloidal Quantum Dot Solids. *ACS Nano* **2012**, *6*, 8448−8455.

(21) Zunger, A. Practical Doping Principles. *Appl. Phys. Lett.* **2003**, *83*, 57.

(22) Moreels, I.; Fritzinger, B.; Martins, J. C.; Hens, Z. Surface Chemistry of Colloidal PbSe Nanocrystals. *J. Am. Chem. Soc.* **2008**, *130*, 15081−15086.

(23) Voznyy, O. Mobile Surface Traps in CdSe Nanocrystals with Carboxylic Acid Ligands. *J. Phys. Chem. C* **2011**, *115*, 15927−15932.

(24) Erwin, S. Doping PbSe Nanocrystals: Predictions Based on a Trapped-Dopant Model. *Phys. Rev. B* **2010**, *81*, 235433.

(25) Manna, L.; Wang, L.-W.; Cingolani, R.; Alivisatos, A. P. First-Principles Modeling of Unpassivated and Surfactant-Passivated Bulk Facets of Wurtzite CdSe: A Model System for Studying the Anisotropic Growth of CdSe Nanocrystals. *J. Phys. Chem. B* **2005**, *109*, 6183−6192.

(26) Dubowski, J. J.; Voznyy, O.; Marshall, G. M. Molecular Self-Assembly and Passivation of GaAs (001) with Alkanethiol Monolayers: A View Towards Bio-functionalization. *Appl. Surf. Sci.* **2010**, *256*, 5714−5721.

(27) Peng, H.; Song, J.-H.; Kanatzidis, M. G.; Freeman, A. J. Electronic Structure and Transport Properties of Doped PbSe. *Phys. Rev. B* **2011**, *84*, 125207.

(28) Puzder, A.; Williamson, A. J.; Gygi, F.; Galli, G. Self-Healing of CdSe Nanocrystals: First-Principles Calculations. *Phys. Rev. Lett.* **2004**, *92*, 217401.

(29) Del Ben, M.; Havenith, R. W. A.; Broer, R.; Stener, M. Density Functional Study on the Morphology and Photoabsorption of CdSe Nanoclusters. *J. Phys. Chem. C* **2011**, *115*, 16782−16796.

(30) Kilina, S. V.; Ivanov, S.; Tretiak, S. Effect of Surface Ligands on Optical and Electronic Spectra of Semiconductor Nanoclusters. *J. Am. Chem. Soc.* **2009**, *131*, 7717−7726.

(31) Pashley, M. D. Electron Counting Model and Its Application to Island Structures on Molecular-Beam Epitaxy Grown Gaas(001) and Znse(001). *Phys. Rev. B* **1989**, *40*, 10481−10487.

(32) Puzder, A.; Williamson, A. J.; Reboredo, F. A.; Galli, G. Structural Stability and Optical Properties of Nanomaterials with Reconstructed Surfaces. *Phys. Rev. Lett.* **2003**, *91*, 157405.

(33) Osedach, T. P.; Zhao, N.; Andrew, T. L.; Brown, P. R.; Wanger, D. D.; Strasfeld, D. B.; Chang, L.; Bawendi, M. G.; Bulović, V. Bias-Stress Effect in 1,2-Ethanedithiol-Treated PbS Quantum Dot Field-Effect Transistors. *ACS Nano* **2012**, *6*, 3121−3127.

(34) Soler, J. M.; Artacho, E.; Gale, J. D.; Garcia, A.; Junquera, J.; Ordejon, P.; Sanchez-Portal, D. The SIESTA Method for Ab Initio Order-N Materials Simulation. *J. Phys.: Condens. Matter* **2002**, *14*, 2745−2779.

(35) Argeri, M.; Fraccarollo, A.; Grassi, F.; Marchese, L.; Cossi, M. Density Functional Theory Modeling of PbSe Nanoclusters: Effect of Surface Passivation on Shape and Composition. *J. Phys. Chem. C* **2011**, *115*, 11382−11389.

(36) Maksymovych, P.; Voznyy, O.; Dougherty, D. B.; Sorescu, D. C.; Yates, J. T., Jr. Gold Adatom as a Key Structural Component in

Self-assembled Monolayers of Organosulfur Molecules on Au(111). *Prog. Surf. Sci.* **2010**, *85*, 206−240.
(37) Hines, M. A.; Scholes, G. D. Colloidal PbS Nanocrystals with Size-Tunable Near-Infrared Emission: Observation of Post-Synthesis Self-Narrowing of the Particle Size Distribution. *Adv. Mater.* **2003**, *15*, 1844−1849.
(38) Jasieniak, J.; Bullen, C.; van Embden, J.; Mulvaney, P. Phosphine-Free Synthesis of CdSe Nanocrystals. *J. Phys. Chem. B* **2005**, *109*, 20665−20668.
(39) Fritzinger, B.; Capek, R. K.; Lambert, K.; Martins, J. C.; Hens, Z. Utilizing Self-Exchange to Address the Binding of Carboxylic Acid Ligands to CdSe Quantum Dots. *J. Am. Chem. Soc.* **2010**, *132*, 10195−10201.
(40) Moreels, I.; Justo, Y.; Geyter, B. De; Haustraete, K.; Martins, J. C.; Hens, Z. Size-Tunable, Bright, and Stable PbS Quantum Dots: A Surface Chemistry Study. *ACS Nano* **2011**, *5*, 2004−2012.
(41) Owen, J. S.; Park, J.; Trudeau, P.-E.; Alivisatos, A. P. Reaction Chemistry and Ligand Exchange at Cadmium-selenide Nanocrystal Surfaces. *J. Am. Chem. Soc.* **2008**, *130*, 12279−12281.
(42) Cademartiri, L.; Bertolotti, J.; Sapienza, R.; Wiersma, D. S.; von Freymann, G.; Ozin, G. A. Multigram Scale, Solventless, and Diffusion-Controlled Route to Highly Monodisperse PbS Nanocrystals. *J. Phys. Chem. B* **2006**, *110*, 671−673.
(43) Anderson, N. C.; Owen, J. S. Soluble, Chloride-Terminated CdSe Nanocrystals: Ligand Exchange Monitored by ^{1}H and ^{31}P NMR Spectroscopy. *Chem. Mater.* **2013**, *25*, 69−76.
(44) Loken, C.; Gruner, D.; Groer, L.; Peltier, R.; Bunn, N.; Craig, M.; Henriques, T.; Dempsey, J.; Yu, C.-H.; Chen, J.; et al. SciNet: Lessons Learned from Building a Power-Efficient Top-20 System and Data Centre. *J. Phys Conf. Ser.* **2010**, *256*, 012026.